Chemosphere 238 (2020) 124573

Contents lists available at ScienceDirect

Chemosphere

journal homepage: www.elsevier.com/locate/chemosphere

Effect of temperature on toxicity and biodegradability of dissolved organic nitrogen formed during hydrothermal liquefaction of biomass

Sirwan Alimoradi [a], Hannah Stohr [b], Susan Stagg-Williams [b], Belinda Sturm [a, *]

[a] Civil, Environmental, and Architectural Engineering Department, The University of Kansas, Lawrence, KS, 66045, USA
[b] Chemical & Petroleum Engineering Department, The University of Kansas, Lawrence, KS, 66045, USA

HIGHLIGHTS

- Increasing HTL reaction temperature increased the formation of HNOCs.
- The higher the temperature the lower the biodegradability of nitrogen.
- The highest temperature of 345 °C generated ACP with the greatest toxicity.
- An optimal HTL reaction temperature can maximize nitrogen recovery.

GRAPHICAL ABSTRACT

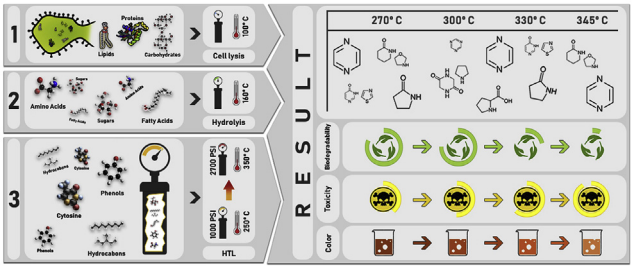

ARTICLE INFO

Article history:
Received 19 March 2019
Received in revised form
19 July 2019
Accepted 10 August 2019
Available online 12 August 2019

Handling Editor: Yongmei Li

Keywords:
Nitrogen recovery
Non-biodegradable dissolved organic nitrogen (nbDON)
Heterocyclic N-Containing organic compounds (HNOCs)
Hydrothermal liquefaction (HTL)
HTL wastewater
Toxicity

ABSTRACT

This study investigated the nutrient content and reuse potential of wastewater generated during hydrothermal liquefaction of microalgal biomass. The hydrothermal liquefaction reaction was tested at 270, 300, 330, and 345 °C to determine the effect of temperature on the formation of non-biodegradable dissolved organic nitrogen (nbDON). Total nitrogen, ammonium, color, and toxicity were selected as key characteristics for the reuse of hydrothermal liquefaction wastewater. Results indicated that a higher concentration of $nbDON_5$ (nbDON defined with a 5 day growth assay) and more diverse heterocyclic N-containing organic compounds were associated with greater toxicity as measured by a growth rate assay. For the tested temperature ranges, the total nitrogen content of the hydrothermal liquefaction wastewater slightly decreased from $5020 \pm 690\ mg\ L^{-1}$ to $4160 \pm 120\ mg\ L^{-1}$, but the % $nbDON_5$ fraction increased from 57 ± 3 %DON to 96 ± 5 %DON. The temperature of hydrothermal liquefaction reactions can be optimized to maximize carbon conversion and nitrogen recovery.

1. Introduction

The potential of algal biofuels has improved with the recent application of hydrothermal liquefaction (HTL), a process that converts minimally dewatered biomass to biocrude. HTL utilizes wet biomass (~10–20% solids) to produce biocrude, solids, gases, and aqueous wastewater. However, maximizing carbon and nutrient recovery is essential for sustainable biofuel production. Biller et al. (2012) showed that a closed loop system using recovered nutrients from the aqueous wastewater for more microalgal

* Corresponding author. 1530 W 15th St, 2150 Learned Hall, Lawrence, KS, 66045.
E-mail address: bmcswain@ku.edu (B. Sturm).

https://doi.org/10.1016/j.chemosphere.2019.124573
0045-6535/

biomass growth offers a promising route for sustainable oil production and nutrient management. Jena et al. (2011) showed that it is possible to cultivate freshwater microalgae *C. minutissima* using the process water of HTL to recycle nitrogen. Therefore, HTL and recycling of the HTL wastewater, which is also called aqueous co-product (ACP), enables a closed loop process that reduces the energy-intensive dewatering step typically associated with algal biofuels and improves nutrient sustainability.

To maximize energy and nutrient recovery, the desired elemental distribution is C in the biocrude, N in the HTL wastewater, and P in the HTL-solids. Previous research converting both mono- and mixed algal cultures has shown that 50% of the carbon in biomass fed to an HTL reactor is recovered in the biocrude, while 95% of the phosphorus can be recovered in the biochar or HTL-solids (Alimoradi et al., 2017; Hable et al., 2019; Roberts et al., 2015). Since the HTL wastewater contains 20–50% of the initial load of organic carbon and a large fraction of the initial organic nitrogen (Pham et al., 2013), reducing the organic carbon and nitrogen loss is critical to the overall economic viability of the process. Nitrogen in the HTL wastewater can be recycled for biomass growth if it remains in a bioavailable form. Reaction temperature is the key parameter that changes the distribution of organics between the HTL products (Xu and Savage, 2017).

The total nitrogen (TN) in HTL wastewater gradually increases with increasing HTL reaction temperature when reaction time is less than 20 min (Choi et al., 2017). Conversely, Choi et al. showed that with increasing reaction temperature and longer reaction times (higher than 40 min), the TN content of HTL wastewater gradually decreases. In addition to reaction time and temperature, the macromolecular composition of the feedstock also affects the HTL product yield and quality. Vardon et al. (2011) performed HTL reactions on *Spirulina* algae, swine manure, and digested municipal sludge, and their results showed that the feedstock macromolecular content impacted yield and the functional groups of the biocrude.

To optimize the HTL system for nutrient and biofuel yield and properties, it is necessary to understand the reaction chemistry for the formation and fate of N-containing compounds during the HTL reaction. During the temperature ramp and holding time, interactions between macromolecules have characteristics similar to the Maillard reaction (Liu et al., 2008; Peterson et al., 2010). The Maillard reaction occurs between the amine groups present in proteins and the carbonyl groups present in carbohydrates. The reaction is initiated by a nucleophilic attack of the non-bonding pair of electrons of the primary amine group of the amino acid on the carbonyl group of the sugar. In the first stage of the Maillard reaction, the products of the sugar and amino acid reaction produce a range of complex compounds. Further increasing the temperature results in a combination of multiple parallel and sequential reactions leading to a broad range of brown, heterogeneous, high molecular weight polymers referred to as melanoidins (Peterson et al., 2010; Wang et al., 2011). Thus, temperature, reaction time, and macromolecular content of the biomass are three main variables that determine the Maillard reactions and its products.

A list of 48 organic compounds that are commonly reported in HTL wastewater includes many heterocyclic N-containing organic compounds (HNOCs) (Pham et al., 2013). The HNOCs can be classified based on the number of membered rings (i.e., 5-membered rings) and the saturation status (saturated or unsaturated). The toxicity of some HNOCs to bacteria (Zhou et al., 2017) and mammalian cells (Pham et al., 2013) has been reported. He et al. (2017) also reported that a fraction of HTL wastewater is non-biodegradable or toxic.

In order to use HTL wastewater as a nutrient source or safely discharge to the environment, HNOCs should be reduced, either during the reaction or by the addition of a pretreatment step. The objectives of this study were to (i) quantify dissolved organic nitrogen (DON) formation in HTL wastewater regarding biodegradability and recalcitrance as a function of HTL reaction temperature, (ii) characterize and quantify the toxicity of HTL wastewater using pure cultures, and (iii) propose a temperature dependency for the formation of HNOCs. This study enables engineers to optimize the HTL reaction temperature to maximize carbon and nitrogen recovery.

2. Materials and methods

2.1. Microalgae growth and characterization

Chlorella kessleri (UTEX #262) was grown in a 1000-L raceway pond (Waterwheel Factory, Franklin, NC, USA) located at the University of Kansas. Tap water was used as the bulk water and modified to BG-11 (Stanier et al., 1971) with an N:P molar ratio of 10. The pH was regulated at 7.4 ± 0.2 by diffusing CO_2 into the system (YSI Incorporated, Yellow Springs, Ohio, USA). Algal biomass was harvested during the stationary growth phase using an Evodos type 10 centrifuge (Evodos, Netherland). The collected algal cake was freeze-dried (LABCONCO, Kansas City, MO) to obtain algal powder less than 10 wt% moisture and stored at 4 °C for biomass characterization and HTL processing.

Table 1 shows the characteristics of the algal biomass used in this study. Ultimate elemental analysis of C, H, N, and O of the dried biomass was measured using a CHNS/O Elemental Analyzer (PerkinElmer 2400 Series II, Waltham, MA). Moisture and ash content of the algal solids were approximated using an SDT Q600 Thermogravimetric Analyzer (TGA) (TA Instruments, New Castle, Pennsylvania, USA). To measure the inorganic elemental content, dried biomass was digested and analyzed using an inductively coupled plasma optical emission spectrometers (ICP-OES, Varian 725-ES, Varian, Australia). Digestion was performed with 0.3 g of algal solid in 6 mL of HNO_3 and 2 mL of HCl using a microwave reaction system (Multiwave PRO, Anton Paar Co., Ashland, VA, USA) at 250 °C for 20 min (500 W, 75 cc PEFT vessels).

Prior to all macromolecular analyses described below, cell lysis was performed in a two-step process. First, the algal solid was sonicated at 50/60 Hz, 2.0 A in a Digital Sonifier 250 (Branson Ultrasonics, Danbury, Connecticut, USA) for three cycles of 5 s sonication and 3 s rest. Second, sodium dodecyl sulfate (SDS) was added at a 2% (v/v) concentration for 30 min, followed by centrifugation, with the supernatant analyzed for macromolecular analyses. The Anthrone method (Davidson and Sackner, 1963) was used to

Table 1
Algal biomass characteristics.

Approximate	(wt%)
Moisture	8.4 ± 0.3[a]
Volatile	57.8 ± 0.5
Combustible	11.6 ± 0.2
Ash content	22.3 ± 0.3
Macromolecular Content	(afdw%)
Carbohydrate	17.3 ± 0.1
Protein	40.9 ± 1.7
Lipid (by FAME)	27.8 ± 3.9
Organic Elements	(afdw%)
Carbon	55.4 ± 0.8
Nitrogen	7.4 ± 0.1
Nitrogen	8.2 ± 0.2
Oxygen (by difference[b])	31.8 ± 0.6

[a] *All ± correspond to standard deviation.*
[b] *Standard deviation for Oxygen calculated from Gaussian error propagation.*

measure the carbohydrate content of the algal solid. The Lowry protein assay (Hartree, 1972) was used to estimate the protein content. Finally, a three-solvent lipid extraction technique was performed for lipid extraction (Barney et al., 2012). Fatty acid methyl esters (FAME) were derived by transesterification according to Laurens et al. (2012). Gas chromatography-mass spectrometry (GC/MS) was used to quantify and qualify the profile of the extracted lipids and FAMEs using a 7890B GC System with a mass spectrometry detector 5977A (Agilent, Santa Clara, CA) (Agilent, Ltd., California, USA) with an Agilent 19091S-433UI:1 HP 5 ms Ultra Inlet column (Agilent, USA), 30 m 250 μm ID and 0.25 μm FT.

2.2. Hydrothermal experimental design

A 450 mL 4560 series mini benchtop reactor attached to a 4848-model controller (Parr, Moline, IL, USA) was used to perform the HTL reactions. The reactor was charged with 30 g of freeze-dried algal solid and 270 mL of Milli-Q water to make a 10 wt% algal slurry. The temperature was ramped at a rate of 5.0 ± 0.5 °C/min to reach the final temperatures of 270, 300, 330, and 345 °C, with corresponding approximate pressures of 800, 1200, 1900, and 2300 psi. The reactor was constantly stirred at a rate of 150 rpm, and the final temperature was held for 1 h.

2.3. Analytical methods

2.3.1. Wastewater recovery from HTL

Post-reaction, the reactor was cooled immediately, and HTL wastewater was collected by centrifugation of the reactor contents at 5000 rpm for 4 min. Following centrifugation, the HTL wastewater was filtered through 0.45 μm filter and stored in the dark at room temperature with no headspace.

2.3.2. Liquid–Liquid extraction

For identification purposes, compounds in the HTL wastewater were extracted using published methods (Pham et al., 2013). Briefly, the HTL wastewater was first made alkaline (pH higher than 13) using NaOH. Then, 50 mL of dichloromethane (DCM) was added to 2.5 mL of the alkaline HTL wastewater. The mixture was loaded into a 125 mL separatory funnel and shaken gently for 1 min to extract the HNOCs. The DCM layer was collected after 5 min as the first extract. The emulsion was recovered and adjusted to a pH of 5 using 6 M HCl. The pH-adjusted emulsion was transferred back into the separatory funnel, and it was further extracted with another 50 mL of DCM. The DCM layer was collected as the second extract. Lastly, a solid phase extraction was performed on the recovered supernatant from the second extraction using a Sep-Pak tC18 Plus Long Cartridge (Waters Associates, Milford, MA). The absorbed sample was extracted from the cartridge by 10 mL of DCM as a third extract. The three extracted HTL wastewater (HTL-WW_{ext}) parts were combined and analyzed by GC/MS.

2.3.3. Gas chromatography and mass spectrometry analyses

Identification and quantification of extracted compounds were conducted with a 7890B GC System with mass spectrometry 5977A (Agilent Technology, Santa Clara, CA). Separation was accomplished with an Agilent 19091S- column (30 m × 0.25 mm × 0.25 μm) with helium at a flow rate of 1.0 mL/min. A 1 μL dose of the HTL-WW_{ext} was injected at 270 °C at a split ratio of 1:1. The temperature ramp was created from published methods (Pham et al., 2013). Extracted compounds were identified by using a NIST 11 mass spectral library (NIST/EPA/NIH mass spectral library, 2011 edition). It should be noted that isomers of a compound were aggregated (e.g., methyl isomers of pyrazines were included in the pyrazine concentration). A 100 ppm 1-chlorooctane dose was added to HTL-WW_{ext} samples as an internal standard for estimating concentrations. The high diversity of compound structures, along with their isomers, made it hard to quantify each compound utilizing external-standards.

2.4. Color measurement

The HTL wastewater color was analyzed for absorbance over the range of 390–700 nm at a scan rate of −300 nm/min with a data interval of 0.5 nm (Peterson et al., 2010) by a BioTek™ Eon™ Microplate Spectrophotometer (Vermont, USA). Absorbance at wavelength 420 nm (A_{420}) was reported explicitly as an indicator of brown color (Liu et al., 2008). In addition, step by step (1 + 1 by vol) HTL wastewater + MilliQ-water dilution was performed at A_{420} to calculate a color dilution (CD) factor (Hofmann, 1998). The CD factor is defined as the dilution of the sample at which the color is just detectable visually in a cuvette test tube using water as the blank. In the modified approach used here, the dilution at which the second derivative of the non-linear regression formula is equal to zero is defined as the CD factor. The approach is defined by equations (1) and (2):

$$Color\ Dilution\ Factor\ (CD) = 2^{\alpha} \tag{1}$$

$$When \quad \frac{d^2 f(A_{420})}{d\alpha^2} = 0 \tag{2}$$

where, $f(A_{420})$ is the nonlinear regression formula of the absorbance data at wavelength 420 nm after each dilution, and α is the dilution step at which the nonlinear formula is equal to zero.

2.5. EC_{50} toxicity

The 50% effective concentration (EC_{50}) reflects the concentration of HTL wastewater that produced a 50% reduction in the maximum growth rate of *Bacillus subtilis* when incubated for 24 h at 37 °C. A range of HTL wastewater dilutions was evaluated, from 1% to 10% (v/v). Since HTL wastewater contains ammonium, the MOPS media (Neidhardt et al., 1974) was modified by adding different concentrations of ammonium for each HTL wastewater, to make a constant ammonium concentration of 2300 mg-N/L in all samples. A BioTek™ Eon™ Microplate Spectrophotometer (Vermont, USA) was used to inoculate 96-wells with 8 different HTL wastewater dilutions to monitor the growth curves. Optical density measurements were taken at 650 nm every 15 min. The optical density data was then analyzed by logistic regression (Eq. (3)) to find the maximum rate of growth (r_{max}) for each HTL wastewater concentration (12 replicates for each). dN/dt is the specific growth rate, K is the carrying capacity, and N is the population size.

$$\frac{dN}{dt} = r_{max}\left(\frac{K-N}{K}\right)*N \tag{3}$$

$$r_{max} = r_{bottom} + \frac{(r_{top} - r_{bottom})}{1 + \left(\frac{\%HTL-WW}{EC_{50}}\right)^{-n}} \tag{4}$$

$$Fit\% = \frac{1 - \sum(r_{measured} - r_{modeled})^2 \Big/ n^{0.5}}{maximum\ of\ r_{measured}} \tag{5}$$

Then, using those r_{max} for each HTL wastewater dilution (1%–10%), the least squares method was applied to estimate the parameters of the Hill inhibition equation (Eq. (4)). r_{bottom} is the smallest observed r_{max}, r_{top} is the highest observed r_{max}, %HTL-WW is the dilution tested as percent HTL wastewater by volume, and n is

the Hill coefficient, which governs the slope of the inhibition function and describes the time-dependency of inhibition (Keymer et al., 2013; Weiss, 1997). R programming was used to find the best numerical fit (maximum % Fit) (Eq. (5)) for a range of possible EC_{50} (1–10) and n coefficient (−3 to 0) values. The Hill equation has been widely used to analyze quantitative drug–receptor relationships in pharmacology (Goutelle et al., 2008). The more negative the n coefficient, the steeper the curve shape is. Together, the combination of EC_{50} (concentration-dependent) and Hill coefficient n (time-dependent) can quantitatively describe the possible toxicity (inhibition) within the structure of the Hill equation (Goutelle et al., 2008).

2.6. Nitrogen characterization

After the HTL reaction, total organic carbon (TOC), total nitrogen (TN), and ammonium of HTL wastewater were measured. A Torch Combustion TOC/TN Analyzer (Teledyne Tekmar, Waltham, MA) was utilized for TOC and TN measurements. Ammonium was measured using the Phenate method *(Standard Methods* 4500-NH3 F) and read at 580 nm wavelength (Rice et al., 2012). Nitrate (NO_3^-) and nitrite (NO_2^-) were analyzed by ion chromatography (Dionex ICS-2000, USA). The total DON concentration was calculated by subtracting inorganic N (ammonium, nitrate, and nitrite) from TN.

To quantify nbDON in HTL wastewater, a 5-day biological nitrogen uptake ($nbDON_5$) experiment was conducted. MOPS nutrient growth media was modified to include only 0.5% or 1% HTL wastewater as the sole N source (the N-containing buffers, tricine, and ammonium were omitted), which was used to grow *Escherichia coli* (*E. coli*) and *Pseudomonas putida (P. putida)* based on a study by Nelson et al. (2013). *E. coli* was chosen since it has been widely used in industrial processes as a model microorganism. Heipieper et al. (1992) indicated that *P. putida* responded to sub-lethal concentrations of phenol by increasing the degree of saturation in the fatty acid composition of the lipids in the cell membrane, thus providing membrane permeability and minimizing the impact of the toxic substances. The bacteria were grown in triplicate for each HTL wastewater dilution (0.5% and 1.0%) for 5 days at 37 °C while being constantly shaken at 120 rpm. The pH of the media was adjusted to 7.4 ± 0.1 before inoculation. At the end of the 5-day period, the samples were centrifuged at 10,000 rpm for 2 min and filtered through a 0.22 μm filter to collect the supernatant. Samples were then analyzed to identify the post-growth concentrations of TN, TOC, and ammonium (duplicate measurement). ICP-OES was used to measure (triplicate) the elemental content of the supernatant to test if there were any limiting elements, other than nitrogen. The $nbDON_5$ and $bDON_5$ (biodegradable dissolved organic nitrogen) were calculated using equations (6) and (7).

$$nbDON_5 = (TN_{PG} - Ammonium_{PG}) * ACP\ dilution \quad (6)$$

$$bDON_5 = DON_{HTL-WW} - nbDON_5 \quad (7)$$

where TN_{PG} and $Ammonium_{PG}$ are the concentrations of total nitrogen and ammonium in the post-growth supernatant. The $DON_{HTL\text{-}WW}$ is the concentration of the dissolved organic nitrogen in the HTL wastewater, and *ACP dilution* is the dilution factor of the HTL wastewater before starting the 5-day bacterial growth assay.

2.7. Statistical analysis

All TOC, TN, and ammonium samples for HTL wastewater and $nbDON_5$ tests have been measured in triplicate. To test the significant difference between all measurements for varying temperatures, one way ANOVA statistical analysis has been performed at the significance level of 0.05 based on Tukey means comparison approach. Standard deviations for the three ICP measurements and bDON were calculated based on values from Gaussian error propagation.

3. Results and discussion

3.1. HTL wastewater yield and characterization

Two primary concerns for recycling or treating HTL wastewater are the biodegradability of N compounds and their toxicity. To evaluate N management options, the yield and composition of the HTL wastewater need to be determined. For all four HTL reaction temperatures, HTL wastewater recovery was >96% when compared to the input water.

The results for TOC showed a decrease from 16000 ± 570 to 8300 ± 150 mg L^{-1} when the reaction temperature increased from 270 °C to 345 °C. The p-value for ANOVA test was significant ($p < 0.05$, ANOVA) between all temperatures, except 330 and 345 °C. Decomposition of the melanoidins, which increases the formation of water-insoluble organic compounds (Minowa et al., 2004), begins at 200 °C and continues up to temperatures near 350 °C. Our results showed that organic partitioning from the aqueous phase to the oil phase reached its maximum at 330 °C. Increasing the temperature from 270 °C to 345 °C decreased the C content of the HTL wastewater from 19% to 10% of the initial C in the biomass. Yu et al. (2011) measured TOC at temperatures higher than 220 °C and retention times longer than 10 min. They reported an increase in C recovery in the HTL wastewater up to 40% of the initial C in the biomass until a temperature of 260 °C, then a decrease to 30% at a temperature of 300 °C when a 30-min retention time was applied. In contrast to our results, Biller et al. (2012) observed that an increase in temperature from 300 °C to 350 °C resulted in an increase from 11000 to 14000 mg L^{-1} TOC content in the HTL wastewater for *Chlorella*. They described the increase as greater decomposition of organic compounds into polar organics. This decomposition consequently reduced the polar organic compounds in the biocrude. However, the concentration of TOC in the HTL wastewater varied between 9000 and 15000 mg L^{-1} for different algal feedstocks and reactions (Biller et al., 2012). In two other publications (Chen, 2018; Yu et al., 2011), a tradeoff between C recovery in the HTL wastewater and biocrude was established with increased temperature resulting in increased biocrude yield and decreased TOC in the HTL wastewater. Our data is in accordance with these findings.

Similar to TOC results, TN in the HTL wastewater decreased from 5100 ± 690 to 4200 ± 120 mg L^{-1} ($p < 0.05$, ANOVA) when the temperature increased from 270 °C to 345 °C (Fig. 1a). The percent nitrogen recovery in the HTL wastewater changed from 73% to 60%. Our results are similar to the Yu et al. (2011) findings, which show that although nitrogen recovery in the HTL wastewater increases with increasing temperature, the rate of change for nitrogen recovery in the HTL wastewater slows down at temperatures above 240 °C, with maximum TN concentrations at 280 °C. The result implies that the majority of nitrogen in the initial biomass will be converted into water-soluble products by increasing the reaction temperature up to 280 °C. In our results, the TN decrease from 270 °C to 345 °C can be interpreted similarly to the TOC decrease, with more water-insoluble or polar compounds being produced at higher temperatures, resulting in more TN partitioning to the oil phase versus the HTL wastewater (Yu et al., 2011). Possible partitioning to the gas phase was not measured in this study.

The total inorganic nitrogen of HTL wastewater contains ammonium, nitrate, and nitrite. The ammonium concentration increased from 2160 ± 30 to 2490 ± 20 mg L^{-1} when the reaction

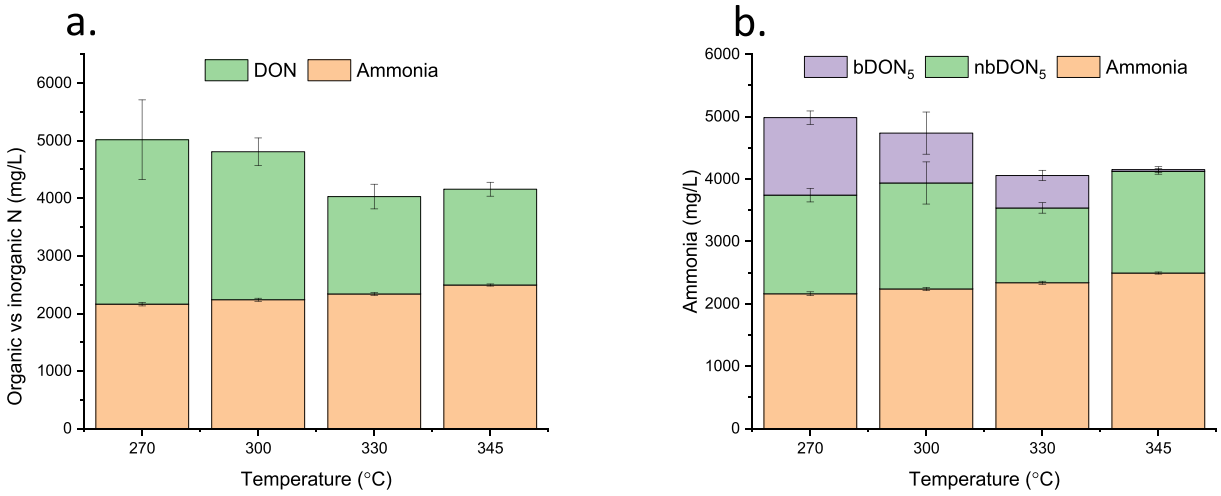

Fig. 1. a. Concentration of ammonium and dissolved organic nitrogen (DON) in the HTL wastewater performed at temperatures of 270, 300, 330, and 345 °C using P. putida for the bio-assay; b. Concentration of ammonium, $bDON_5$, $nbDON_5$, and nitrate in the HTL wastewater. Error bars are standard deviations of three measurements for TN, ammonium, and $nbDON_5$. Error bars for bDON5 are calculated from Gaussian error propagation.

temperature increased from 270 °C to 345 °C ($p < 0.05$, ANOVA). Biller et al. (2012) also reported an increase in ammonium concentration from 6636 to 6888 mg L^{-1} for hydrothermal conversion of *Chlorella* for temperatures of 300 °C and 350 °C, respectively. Other inorganic forms of nitrogen (nitrate and nitrite) were approximately 1% of the TN. Ion chromatography (IC) for all HTL wastewaters showed a non-detect concentration for nitrite (NO_2-N), which was also reported by He et al. (2015). The IC data for nitrate in HTL wastewater for all four reactions were between 30 and 40 mg L^{-1}. He et al. (2015) reported a decrease in nitrate concentration down to 42.3 mg L^{-1} with increasing temperature from 200 °C to 340 °C.

Since ammonium was the dominant inorganic nitrogen species in the HTL wastewater, subtracting ammonium from TN is an appropriate estimate of the dissolved organic nitrogen (DON) concentration. Fig. 1a shows the decrease in DON from 2850 ± 690 to 1690 ± 210 mg L^{-1} with increasing temperature from 270 °C to 330 °C (deviations calculated based on Gaussian error), with a small decrease to 1660 ± 120 mg L^{-1} from 330 to 345 °C. Similar to TOC, these results are consistent with the water-insolubility of organic compounds reaching a maximum at 330 °C. He et al. (2015) reported a 58% decrease in DON with increasing reaction temperature from 200 °C to 260 °C, with smaller reductions in DON from 260 °C to 320 °C. Their results align with our explanation that organic N-containing compounds mostly decompose below 260 °C, and between 260 °C and 320 °C decomposition of N-containing compounds is slower.

The biodegradability of DON depends upon the chemical structure and diversity of the compounds in HTL wastewater. A comprehensive approach to classifying nonbiodegradable and biodegradable DON (nbDON and bDON) is discussed in the following section. As a consequence of increasing the HTL reaction temperature and pressure, the distribution of nitrogen species in the HTL wastewater was greatly altered.

3.2. Biodegradability of dissolved organic nitrogen

The chemical composition of DON affects the bioavailability of DON to bacteria (Liu et al., 2011). Some forms of DON, such as free amino acids, can be readily bioavailable for direct algal uptake, while other forms are bioavailable after bacterial degradation. DON can become more bioavailable to algae through hydrolysis and/or mineralization by bacteria (Simsek et al., 2013).

A 5-day biological nitrogen uptake ($nbDON_5$) experiment was conducted on triplicate batches each of *E. coli* and *P. putida*. Pure cultures were used as model organisms for activated sludge and were used to provide consistency for batch studies performed over several months, since the community structure of full-scale

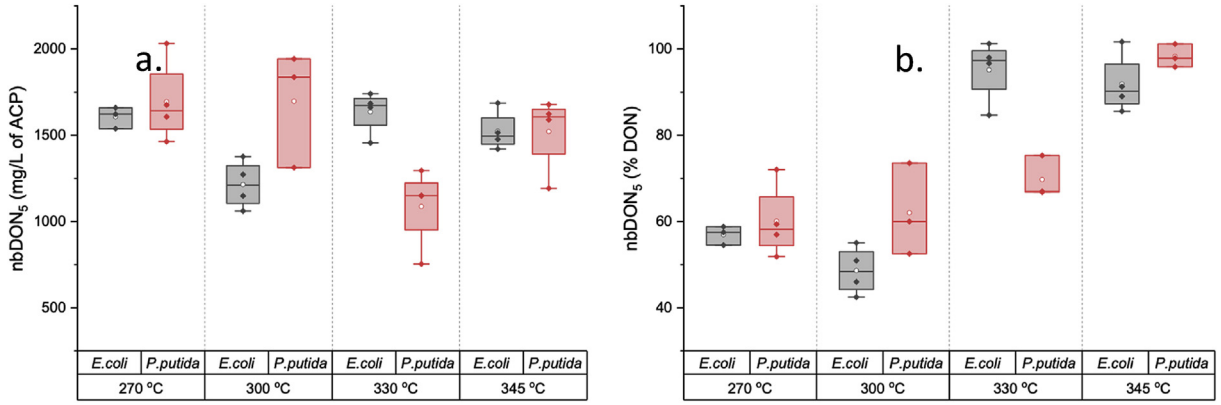

Fig. 2. (a) mg L^{-1} nbDON in HTL wastewater or aqueous co-product (ACP) using two different pure cultures for the bio-assay; and (b) % DON in the ACP that is non-biodegradable.

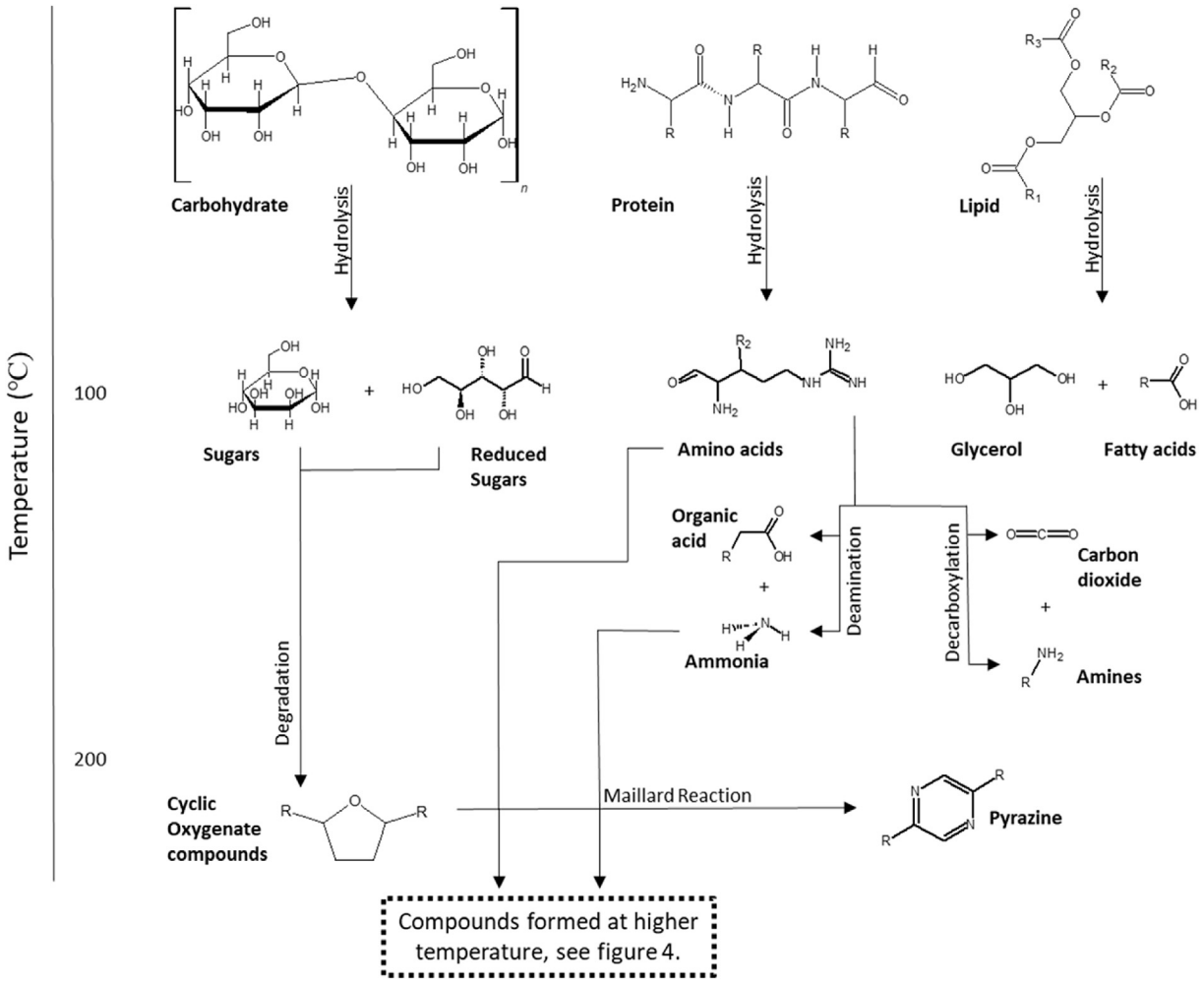

Fig. 3. Brief reaction pathways for HTL of lipid, carbohydrate, and protein macromolecules in the feedstock. For HNOC compounds formed at higher temperatures, see Table 2.

activated sludge varies with time. From an operational standpoint, measuring the concentration of non-biodegradable DON over five days in the HTL wastewater provides an estimate for the amount of N that is unlikely to be recycled within the hydraulic residence time of an algal growth or activated sludge system. In order to estimate the ultimate nbDON fraction, a thirty-day batch study should be considered using a mixed activated sludge community, the results reported herein are limited to a 5-day assay and are denoted as $nbDON_5$. Two different HTL wastewater dilutions (1% and 0.5%) were evaluated for each HTL wastewater produced at the different reaction temperatures. The concentration of the ammonium in each solution was 22.3 ± 2.2 and 11.2 ± 1.1 mg L^{-1} for the 1% and 0.5% HTL wastewater, respectively. The p value between dilutions was not significant ($p > 0.6$, ANOVA). After the microorganisms assimilate all of the biodegradable N, the remaining N is considered non-biodegradable N. Fig. 1b shows the average concentration of $nbDON_5$ in the HTL wastewater based on *P. putida*. Results indicated $nbDON_5$ concentrations of 1580 ± 110, 1700 ± 330, 1200 ± 80, and 1630 ± 50 mg-N L^{-1} for HTL temperatures of 270 °C, 300 °C, 330 °C, and 345 °C. However, $bDON_5$ decreased from 1240 ± 110 to 30 ± 40 mg-N L^{-1} with increasing temperature from 270 °C to 345 °C ($p < 0.05$). Therefore, increasing the HTL reaction temperature from 270 °C to 345 °C caused an increase in percentage of DON attributed to $nbDON_5$ from 56 ± 4 to 98 ± 7 %DON.

Fig. 2 is a box plot of concentrations of $nbDON_5$ in the HTL wastewater for *E. coli* and *P. putida*. *E. coli* was tested as a second species to further demonstrate the 5 day bioassay. The $nbDON_5$ concentration for *E. coli* was in same range at reaction temperatures of 270 °C and 345 °C as *P. putida* and was slightly lower (49 ± 3% DON compared to 67.9 ± 13% DON for *P. putida)* at a reaction temperature of 300 °C. At 330 °C, the $nbDON_5$ for the *E. coli* was significantly higher than the value of $nbDON_5$ measured by *P. putida*. The linear increase of $ndDON_5$ for *P. putida* compared to the *S-shape* increase for *E. coli* can be a result of the relative inhibitory effects on the two species. *P. putida* has demonstrated the ability to adapt their cell lipid structure in response to toxic environments (Heipieper et al., 1992).

3.3. N-containing heterocyclic compounds

The suitability of the HTL wastewater for recycle and recovering nitrogen for biomass growth, depends on the compounds contained within HTL wastewater and understanding the chemical structure, concentration, and diversity. Previous efforts have tried to address HNOC formation during HTL (Gai et al., 2015b; Pham et al., 2013; Sheng et al., 2018). At temperatures around 100 °C, proteins, lipids, and carbohydrates begin hydrolyzing into smaller units, including amino acids, fatty acids, and sugars (Fig. 3). In addition to the reaction between proteins and carbohydrates, which produces HNOCs through the Maillard reaction (Zhang et al.,

Table 2
N-containing Heterocyclic compounds detected in extracted ACP.

	3-Atom Ring	4-Atom Ring	5-Atom Ring		6-Atom Ring		7-Atom Ring
Saturated	Aziridine 	Azetidine 	Pyrrolidine 	Pyrrolidinone 	Piperidine 	Piperidinone 	
			Oxazolidine 	Proline 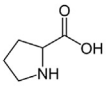	Piperazinedione 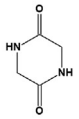	Barbiturate 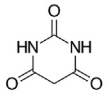	
Unsaturated			Pyrazole 	Triazole 	Pyrimidine 	Pyrazine 	Azepine 
			Thiazole 		Triazine 	Pyrimidone 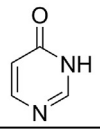	

Table 3
An effective concentration that reduces 50% of the maximum rate of growth (EC50) for P. putida for HTL reactions performed at temperatures of 270, 300, 330, and 345 °C.

Temperature	Main HNOCs[a]	Toxicity measurement	
°C	number	% ACP EC_{50}	Hill Coef. (n)
270	7	6.8 (91.6%[b])	−0.30 (91.6%)
300	8	5.3 (93.9%)	−1.5 (93.9%)
330	10	4.4 (81.8%)	−0.12 (81.8%)
345	11	1.0 (90.5%)	−0.36 (90.5%)

[a] *Number of dominant groups of N-containing heterocyclic compounds.*
[b] *Percent fit based on* equation (5).

2016), HNOCs can be formed as a result of interactions between lipids and proteins. The amino acids from proteins and fatty acids from lipids react to produce esters, amides, and HNOCs (Gai et al., 2015a). Sheng et al. (2018) tested HNOC production in HTL using different model compounds. The mixture of protein and carbohydrate model compounds resulted in producing HNOCs as high as 58.6 wt% (mass dry weight) of the HTL biocrude compounds. Conversely, HTL reactions of mixtures of lipid and protein model compounds resulted in 18.1 wt% HNOCs.

Supplementary information (Table S1) reports the 104 compounds that were identified in this study by GC-MS after DCM extraction of the HTL wastewater. Table 2 shows the main substructure of HNOCs detected in the HTL wastewater for all four HTL temperatures. The GC-MS results for the main HNOCs shows that increasing the HTL reaction temperature from 270 °C to 345 °C, increased the diversity of HNOCs from 7 to 11 (Table 3). The saturation and diversity in number of rings also increased with increasing temperature (Fig. 4). By increasing the temperature from 270 °C to 300 °C, the prevalence of amino acid residue decreased, but some compounds remained unaffected (Supplementary data Table S1). Further increasing the temperature, additional HNOCs with 5-membered rings were detected at 330 °C and 345 °C. At the higher temperatures of 300–375 °C, proteins start to break down, producing cyclic dipeptides and amino acid side chains by pyrolysis-like reactions. Products from the reaction between proteins and carbohydrates include alkyl-pyrrolidinones, pyrazines, pyrroles and melanoidin-like materials (Torri et al., 2012). In addition to the reaction of carboxyl groups and amino acids to produce HNOCs, fatty acids can react with amines to produce amides. Amides can then initiate a reaction to form more HNOCs, such as pyrrolidine derivatives of fatty acids and quinolone derivatives.

Sugars and reducing sugars degrade to cyclic oxygenated compounds around 200 °C (Gai et al., 2015a). The cyclic oxygenated compounds react with ammonium to produce pyrazines (Fig. 3). Increasing the temperature results in a combination of multiple parallel and sequential reactions which generates a broad range HNOCs (Fig. 4). Zhang et al. (2016) reported that when compared with individual proteins, the biocrude derived from the mixture of glucose and proteins contained more pyrazines. In the GC-MS results, pyrazines (with one-, two-, and three-methyl groups) had the highest concentration for all reactions (Fig. 4). From 270 °C to 345 °C, the pyrazine concentration was approximately 400–600 ppm. Pham et al. (2013) found that compounds with more methyl groups are more toxic to algal cell growth.

3.4. Toxicity of HTL wastewater compounds

More knowledge about the HTL wastewater compounds will provide information to minimize the production of non-biodegradable and toxic compounds and guide recycling and treatment strategies. Aruoja et al. (2011) studied the toxicity of 28

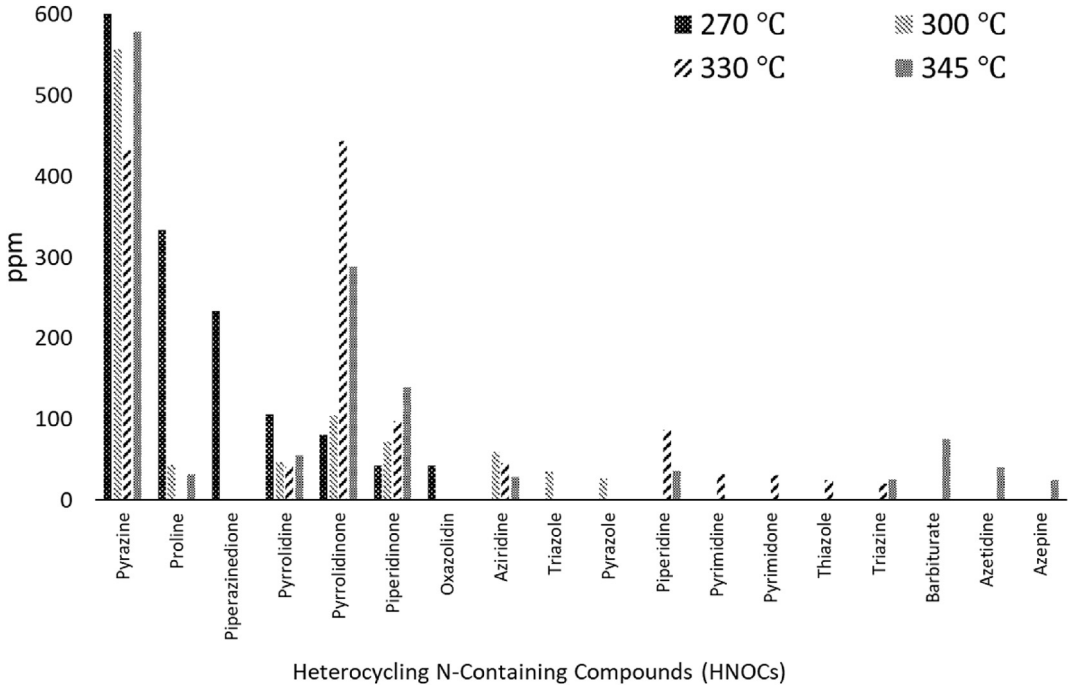

Fig. 4. The GC-MS results of concentration of HNOCs extracted from aqueous co-product of hydrothermal liquefaction for temperatures of 270, 300, 330, and 345 °C.

anilines on the *Pseudokirchneriella subcapitata* using a 72-h algal growth inhibition assay. Anilines were found to be toxic to the cell growth with EC_{50} ranging from 1.43 mg L^{-1} to 109 mg L^{-1}, while eleven compounds had an EC_{50} value less than 10 mg L^{-1}. The inhibitory effects of nine nitrogenous compounds on algal growth have been reported ranging from 0.052 to 139 mg L^{-1} (Pham et al., 2013). Our results showed the presence of five compounds that Pham et al. (2013) also tested: *2,2,6,6-tetramethyl-4-piperidone; 2,6-dimethyl-3pyridinol; pyridine; 1-methyl-2-pyrrolidinone; 2-pyrrolidinone*. Synergistic toxicity effects among these components were also reported by Pham et al. Based on a possible synergistic cytotoxicity effect among the HNOCs, it is necessary to evaluate the toxicity of a mixture of compounds in the HTL wastewater rather than single compounds.

The toxicity of HTL wastewater was measured using the effective concentration that reduces 50% of the maximum rate of growth (EC_{50}) for *P. putida*. The EC_{50} was 6.8, 5.3, 4.4, and 1.0% HTL wastewater (mL HTL wastewater diluted by mL DI water) for HTL reaction temperatures of 270 °C, 300 °C, 330 °C, and 345 °C, respectively (Table 3) ($p < 0.05$, ANOVA). The % HTL wastewater results for EC_{50} correspond to a concentration of 100, 50, 55, 13 mg L^{-1} of extracted HNOCs. In addition, the Hill equation coefficient (n) showed that the greatest acute toxicity might occur at 300 °C since the n was −1.5, which exhibited a steep toxicity response (Table 3). For other temperatures, the Hill coefficient was between 0 and -1, showing a flatter *S* curve behavior when measuring EC_{50}. The negative sign of Hill coefficient (n) describes the negative effect of HTL wastewater on *B. subtitlis* growth rate, showing the inhibitory effect of HNOCs on bacterial growth.

The concentration of phenolic compounds in the HTL wastewater was measured based on GC-MS data in the Supplementary Information (Table S1) as 90, 63, 126, and 208 mg L^{-1} for HTL reaction temperatures of 270, 300, 330, and 345 °C, respectively. These concentrations are higher than those reported by Jena et al. (2011) for thermochemical liquefaction of *S. platensis*. The formation of phenols has been ascribed to the depolymerization and repolymerization reactions that occur during the HTL reaction and the higher phenol concentration observed in this study could be due to the differences in the macromolecular composition of the biomass feedstock. Scragg (2006) studied the effect of phenols on *Chlorella vulgaris* and *Chlorella* VT-1 growth. The initial growth was inhibited with concentration of phenols greater than 100 mg L^{-1}. The sharp increase of EC_{50} in our data at the temperature of 345 °C can be explained by a phenol concentration of 200 mg L^{-1}, two times higher than the inhibitory concentration of 100 mg L^{-1} in the Scragg (2006) study. Another study by Nakai et al. (2001) indicated that it is not just the concentration of phenol but also the type of phenol that has inhibitory effects.

3.5. HTL wastewater color

The results of three different measurements for the color of HTL wastewater are shown in Table 4 and Fig. 5. The HTL wastewater samples had a yellow to brownish color that could be due to the TOC or, more specifically, the presence of HNOCs. Melanoidins, which are produced by the Maillard reaction, have been known to add brown color to food and drinks. The absorption intensity data for the range of 390–700 nm showed that the HTL wastewater color for 270 °C was more intense, with higher absorption throughout the entire tested range (Fig. 5). The A_{420} nm for 270 °C was 1.8 ± 0.4, which was higher than other reaction temperatures (Table 4) ($p < 0.05$, ANOVA).

Table 4
Color measurement based on color dilution factor (CD) and absorption at 420 nm.

Reaction Temperature	Color measurement			
	Color Dilution Factor		Absorption @ 420 nm	
°C	Dilution	CD	Avg.	Std.
270	10	1024	1.8	0.40
300	9	512	1.5	0.01
330	9	512	1.3	0.14
345	8	256	1.3	0.30

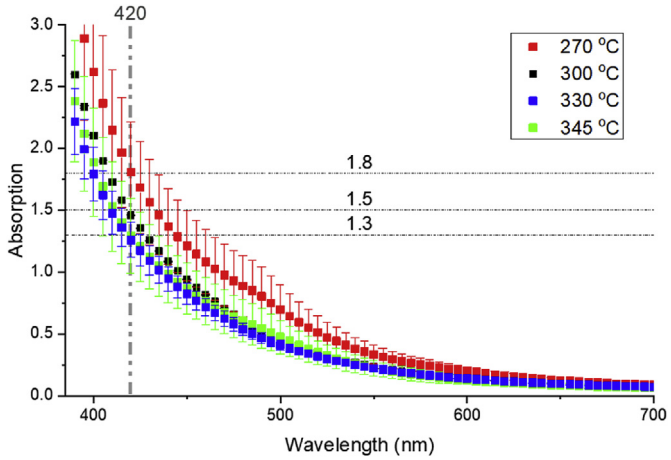

Fig. 5. The absorption intensity of the HTL wastewater over the range of 390–700 nm; the absorbance at wavelength 420 nm (A_{420}) is also specified.

Color intensity was also measured by the color dilution method (CD factor). The results for 12 steps of dilution showed that the CD factor for the HTL wastewater produced from a reaction temperature of 270 °C was also higher than the other reaction temperatures (Table 4). The reduction in color with increased temperature may be explained by the decomposition of melanoidins with increasing temperatures, but it should be noted that all HTL wastewater solutions had significant color, which would have UV transmittance impacts if being disinfected.

3.6. Sankey diagram of the N mass flow

It is estimated that in the U.S., the production of microalgae to replace all transportation fuels would increase the current nitrogen fertilizer demand by 400%, assuming the nutrient source was fertilizer (Pate et al., 2011). Based on our data, at 345 °C, the concentration of 1600 mg L^{-1} of $nbDON_5$ represents 20% of the total initial N in the biomass. Considering HTL wastewater as a source of nutrients for recycling inside the biomass production system, losing 20% of raw material (N fertilizer) is a severe drawback, and the nbDON needs to be minimized for biofuel production with HTL to be sustainable. Different strategies can be considered to minimize the amount of N in the biocrude and biosolids and maximize the biodegradability of N.

Fig. 6 shows the Sankey diagram of N mass flow in HTL wastewaters produced from different reaction temperatures. Based on the ash free dry weight nitrogen content of algal biomass (7.4 ± 0.1 afdw%), the moisture content (8.3 ± 0.3%), and the loading of algae into the reactor (30 g of algae), 2.17 g of N was loaded into the reactor (Table 1). From the N speciation data for each HTL wastewater, the Sankey diagrams show the fate of N to different HTL product phases. The HTL wastewater contains 62.3 ± 5.5, 59.7 ± 2.5, 50.1 ± 2.4, and 51.7 ± 0.1% N of the total N input for temperatures of 270, 300, 330, and 345 °C, respectively (all are statistically different with $p < 0.05$) (Fig. 6). The gradual decrease of the N in the HTL wastewater is based on the production of more water-insoluble organic compounds, which end up in biocrude (Minowa et al., 2004). For ammonium, there was a slight increase from 26.9 ± 0.4 to 31.0 ± 0.2 %N of the total N input. Increasing the temperature caused further degradation of melanoidins to ammonium. The DON portion decreased from 35.5 ± 5.5 to 20.6 ± 0.2 %N of the total N input (Fig. 6). However, in terms of biodegradability of the DON fraction, the bDON decreased from 15.7, 16.6, 3.6, and 0.8% N of the total N input for temperatures of 270, 300, 330, and 345 °C, respectively (Fig. 6).

4. Conclusions

Experimental results from a 5-day bacterial bioassay have

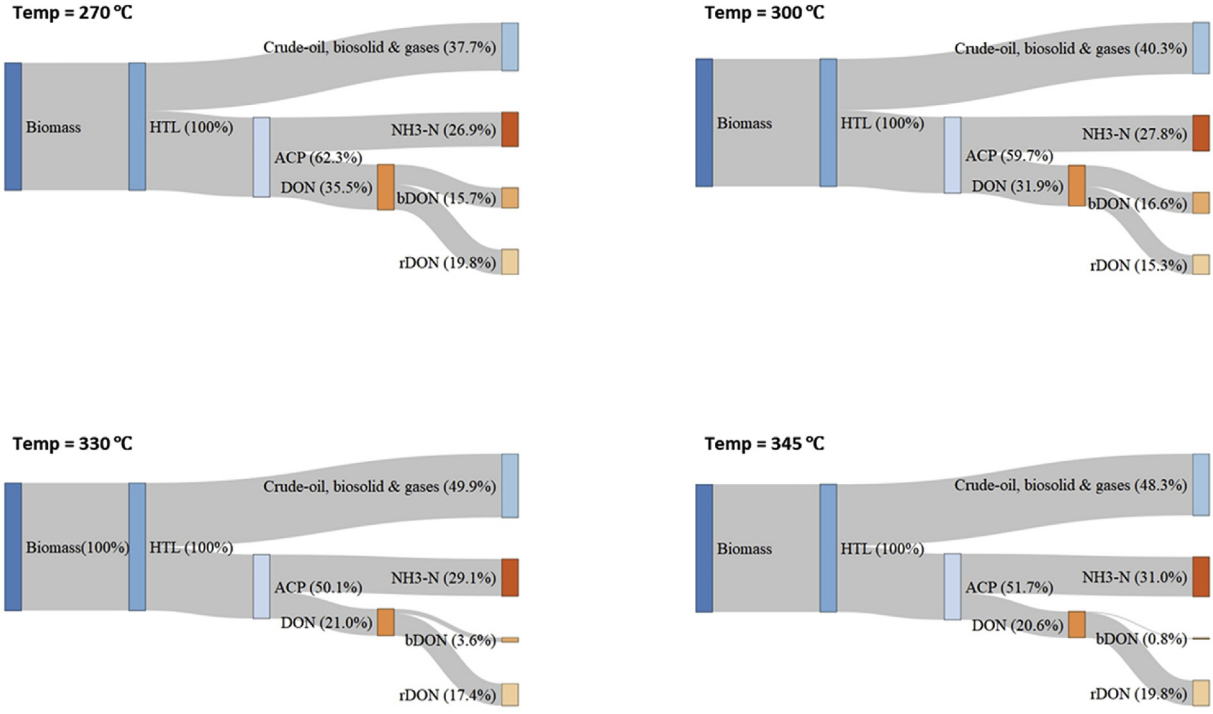

Fig. 6. Sankey diagrams showing the N mass flows (%) to the biocrude, biosolid, and gas phase versus the ACP phase for each of the four HTL reaction temperatures: a) 270 °C; b) 300 °C; c) 330 °C; and d) 345 °C.

shown that the $nbDON_5$ concentration increased from 1200 ± 30 to 1600 ± 60 mg-N L^{-1} as the reaction temperature increased from 300 to 345 °C. The diversity of HNOCs also increased from 7 to 11, and the toxicity regarding EC_{50} increased seven-fold as temperatures ranged from 270 to 345 °C. The results proved the feasibility and potential of reducing HTL reaction temperature to maximize the bioavailability of N in the HTL wastewater. If the temperature of the HTL reaction is reduced to optimize nutrient recovery, the impact on energy production must be considered. Optimization of both energy production and nutrient recovery can increase the economic and environmental sustainability of HTL.

Acknowledgements

This work was supported by the National Science Foundation (NSF CBET-1438652) and a University of Kansas undergraduate research award.

Appendix A. Supplementary data

Supplementary data to this article can be found online at https://doi.org/10.1016/j.chemosphere.2019.124573.

References

Alimoradi, S., Hable, R., Stagg-Williams, S., Sturm, B., 2017. Fate of phosphorous after thermochemical treatment of algal biomass. Proceedings of the Water Environment Federation 2017 (8), 3888–3891.
Aruoja, V., Sihtmäe, M., Dubourguier, H.-C., Kahru, A., 2011. Toxicity of 58 substituted anilines and phenols to algae Pseudokirchneriella subcapitata and bacteria Vibrio fischeri: comparison with published data and QSARs. Chemosphere 84 (10), 1310–1320.
Barney, B.M., Wahlen, B.D., Garner, E., Wei, J., Seefeldt, L.C., 2012. Differences in substrate specificities of five bacterial wax ester synthases. Appl. Environ. Microbiol. 78 (16), 5734–5745.
Biller, P., Ross, A.B., Skill, S., Lea-Langton, A., Balasundaram, B., Hall, C., Riley, R., Llewellyn, C., 2012. Nutrient recycling of aqueous phase for microalgae cultivation from the hydrothermal liquefaction process. Algal Research 1 (1), 70–76.
Chen, J., 2018. Bio-oil production from hydrothermal liquefaction of Pteris vittata L.: effects of operating temperatures and energy recovery. Bioresour. Technol. 265, 320–327.
Choi, D., Lee, J., Tsang, Y.F., Kim, K.-H., Rinklebe, J., Kwon, E.E., 2017. Modification of hydrothermal liquefaction products from Arthrospira platensis by using carbon dioxide. Algal Research 24, 148–153.
Davidson, W.D., Sackner, M.A., 1963. Simplification of the anthrone method for the determination of inulin in clearance studies. Transl. Res. 62 (2), 351–356.
Gai, C., Zhang, Y., Chen, W.-T., Zhang, P., Dong, Y., 2015a. An investigation of reaction pathways of hydrothermal liquefaction using Chlorella pyrenoidosa and Spirulina platensis. Energy Convers. Manag. 96, 330–339.
Gai, C., Zhang, Y., Chen, W.-T., Zhou, Y., Schideman, L., Zhang, P., Tommaso, G., Kuo, C.-T., Dong, Y., 2015b. Characterization of aqueous phase from the hydrothermal liquefaction of Chlorella pyrenoidosa. Bioresour. Technol. 184, 328–335.
Goutelle, S., Maurin, M., Rougier, F., Barbaut, X., Bourguignon, L., Ducher, M., Maire, P., 2008. The Hill equation: a review of its capabilities in pharmacological modelling. Fundam. Clin. Pharmacol. 22 (6), 633–648.
Hable, R.D., Alimoradi, S., Sturm, B.S., Stagg-Williams, S.M., 2019. Simultaneous solid and biocrude product transformations from the hydrothermal treatment of high pH-induced flocculated algae at varying Ca concentrations. Algal Research 40, 101501.
Hartree, E.F., 1972. Determination of protein: a modification of the Lowry method that gives a linear photometric response. Anal. Biochem. 48 (2), 422–427.
He, C., Wang, K., Yang, Y., Amaniampong, P.N., Wang, J.-Y., 2015. Effective nitrogen removal and recovery from dewatered sewage sludge using a novel integrated system of accelerated hydrothermal deamination and air stripping. Environ. Sci. Technol. 49 (11), 6872–6880.
He, Y., Li, X., Xue, X., Swita, M.S., Schmidt, A.J., Yang, B., 2017. Biological conversion of the aqueous wastes from hydrothermal liquefaction of algae and pine wood by Rhodococci. Bioresour. Technol. 224, 457–464.
Heipieper, H.-J., Diefenbach, R., Keweloh, H., 1992. Conversion of cis unsaturated fatty acids to trans, a possible mechanism for the protection of phenol-degrading Pseudomonas putida P8 from substrate toxicity. Appl. Environ. Microbiol. 58 (6), 1847–1852.
Hofmann, T., 1998. Studies on the relationship between molecular weight and the color potency of fractions obtained by thermal treatment of glucose/amino acid and glucose/protein solutions by using ultracentrifugation and color dilution techniques. J. Agric. Food Chem. 46 (10), 3891–3895.
Jena, U., Vaidyanathan, N., Chinnasamy, S., Das, K., 2011. Evaluation of microalgae cultivation using recovered aqueous co-product from thermochemical liquefaction of algal biomass. Bioresour. Technol. 102 (3), 3380–3387.
Keymer, P.C., Pratt, S., Lant, P.A., 2013. Development of a novel electrochemical system for oxygen control (ESOC) to examine dissolved oxygen inhibition on algal activity. Biotechnol. Bioeng. 110 (9), 2405–2411.
Laurens, L.M., Quinn, M., Van Wychen, S., Templeton, D.W., Wolfrum, E.J., 2012. Accurate and reliable quantification of total microalgal fuel potential as fatty acid methyl esters by in situ transesterification. Anal. Bioanal. Chem. 403 (1), 167–178.
Liu, H., Jeong, J., Gray, H., Smith, S., Sedlak, D.L., 2011. Algal uptake of hydrophobic and hydrophilic dissolved organic nitrogen in effluent from biological nutrient removal municipal wastewater treatment systems. Environ. Sci. Technol. 46 (2), 713–721.
Liu, S.-C., Yang, D.-J., Jin, S.-Y., Hsu, C.-H., Chen, S.-L., 2008. Kinetics of color development, pH decreasing, and anti-oxidative activity reduction of Maillard reaction in galactose/glycine model systems. Food Chem. 108 (2), 533–541.
Minowa, T., Inoue, S., Hanaoka, T., MATSUMURA, Y., 2004. Hydrothermal reaction of glucose and glycine as model compounds of biomass. J. Jpn. Inst. Energy 83 (10), 794–798.
Nakai, S., Inoue, Y., Hosomi, M., 2001. Algal growth inhibition effects and inducement modes by plant-producing phenols. Water Res. 35 (7), 1855–1859.
Neidhardt, F.C., Bloch, P.L., Smith, D.F., 1974. Culture medium for enterobacteria. J. Bacteriol. 119 (3), 736–747.
Nelson, M., Zhu, L., Thiel, A., Wu, Y., Guan, M., Minty, J., Wang, H.Y., Lin, X.N., 2013. Microbial utilization of aqueous co-products from hydrothermal liquefaction of microalgae Nannochloropsis oculata. Bioresour. Technol. 136, 522–528.
Pate, R., Klise, G., Wu, B., 2011. Resource demand implications for US algae biofuels production scale-up. Appl. Energy 88 (10), 3377–3388.
Peterson, A.A., Lachance, R.P., Tester, J.W., 2010. Kinetic evidence of the Maillard reaction in hydrothermal biomass processing: glucose– glycine interactions in high-temperature, high-pressure water. Ind. Eng. Chem. Res. 49 (5), 2107–2117.
Pham, M., Schideman, L., Scott, J., Rajagopalan, N., Plewa, M.J., 2013. Chemical and biological characterization of wastewater generated from hydrothermal liquefaction of Spirulina. Environ. Sci. Technol. 47 (4), 2131–2138.
Rice, E.W., Baird, R.B., Eaton, A.D., Clesceri, L.S., 2012. Standard Methods for the Examination of Water and Wastewater. APHA, AWWA, Washington. WPCR 1496.
Roberts, G.W., Sturm, B.S., Hamdeh, U., Stanton, G.E., Rocha, A., Kinsella, T.L., Fortier, M.-O.P., Sazdar, S., Detamore, M.S., Stagg-Williams, S.M., 2015. Promoting catalysis and high-value product streams by in situ hydroxyapatite crystallization during hydrothermal liquefaction of microalgae cultivated with reclaimed nutrients. Green Chem. 17 (4), 2560–2569.
Scragg, A., 2006. The effect of phenol on the growth of Chlorella vulgaris and Chlorella VT-1. Enzym. Microb. Technol. 39 (4), 796–799.
Sheng, L., Wang, X., Yang, X., 2018. Prediction model of biocrude yield and nitrogen heterocyclic compounds analysis by hydrothermal liquefaction of microalgae with model compounds. Bioresour. Technol. 247, 14–20.
Simsek, H., Kasi, M., Ohm, J.-B., Blonigen, M., Khan, E., 2013. Bioavailable and biodegradable dissolved organic nitrogen in activated sludge and trickling filter wastewater treatment plants. Water Res. 47 (9), 3201–3210.
Stanier, R., Kunisawa, R., Mandel, M., Cohen-Bazire, G., 1971. Purification and properties of unicellular blue-green algae (order Chroococcales). Bacteriol. Rev. 35 (2), 171.
Torri, C., Garcia Alba, L., Samori, C., Fabbri, D., Brilman, D.W., 2012. Hydrothermal treatment (HTT) of microalgae: detailed molecular characterization of HTT oil in view of HTT mechanism elucidation. Energy Fuel. 26 (1), 658–671.
Vardon, D.R., Sharma, B., Scott, J., Yu, G., Wang, Z., Schideman, L., Zhang, Y., Strathmann, T.J., 2011. Chemical properties of biocrude oil from the hydrothermal liquefaction of Spirulina algae, swine manure, and digested anaerobic sludge. Bioresour. Technol. 102 (17), 8295–8303.
Wang, H.-Y., Qian, H., Yao, W.-R., 2011. Melanoidins produced by the Maillard reaction: structure and biological activity. Food Chem. 128 (3), 573–584.
Weiss, J.N., 1997. The Hill equation revisited: uses and misuses. FASEB J. 11 (11), 835–841.
Xu, D., Savage, P.E., 2017. Effect of temperature, water loading, and Ru/C catalyst on water-insoluble and water-soluble biocrude fractions from hydrothermal liquefaction of algae. Bioresour. Technol. 239, 1–6.
Yu, G., Zhang, Y., Schideman, L., Funk, T., Wang, Z., 2011. Distributions of carbon and nitrogen in the products from hydrothermal liquefaction of low-lipid microalgae. Energy Environ. Sci. 4 (11), 4587–4595.
Zhang, C., Tang, X., Sheng, L., Yang, X., 2016. Enhancing the performance of Co-hydrothermal liquefaction for mixed algae strains by the Maillard reaction. Green Chem. 18 (8), 2542–2553.
Zhou, M., Yan, B., Wong, J.W., Zhang, Y., 2017. Enhanced volatile fatty acids production from anaerobic fermentation of food waste: a mini-review focusing on acidogenic metabolic pathways. Bioresour. Technol. 248, 68–78.